Anti-parallel β-sheet - a signature structure of the oligomeric amyloid-beta peptide

Emilie Cerf, Rabia Sarroukh, Shiori Tamamizu-Kato, Leonid Breydo, Sylvie Derclaye, Yves Dufrêne, Vasanthy Narayanaswami, Erik Goormaghtigh, Jean-Marie Ruysschaert, Vincent Raussens

ANTI-PARALLEL β-SHEET - A SIGNATURE STRUCTURE OF THE OLIGOMERIC AMYLOID-BETA PEPTIDE.

Emilie Cerf[*¶], Rabia Sarroukh[*¶], Shiori Tamamizu-Kato[†], Leonid Breydo[‡], Sylvie Derclaye[‖], Yves Dufrêne[‖], Vasanthy Narayanaswami[†§], Erik Goormaghtigh[*], Jean-Marie Ruysschaert[*], Vincent Raussens[*].

*: Center for Structural Biology and Bioinformatics, Laboratory for Structure and Function of Biological Membranes, Faculté des Sciences, Université Libre de Bruxelles, CP 206/2, Blvd. du Triomphe, B-1050 Brussels, Belgium.

†: Center for the Prevention of Obesity, Cardiovascular Disease & Diabetes, Children's Hospital Oakland Research Institute, 5700 Martin Luther King Jr. Way, Oakland, California 94609, USA.

[§]Department of Chemistry and Biochemistry, California State University Long Beach, Long Beach, CA 90840, USA.

‡: Department of Molecular Biology and Biochemistry, University of California - Irvine, 3438 McGaugh Hall, Irvine, California 92697, USA.

‖: Unité de Chimie des Interfaces, Université Catholique de Louvain, Croix du Sud 2/18, B-1348 Louvain-la-Neuve, Belgium.

¶ These authors have equally contributed to this manuscript

Address correspondence to: Vincent Raussens, Université Libre de Bruxelles, CP 206/2, Blvd. du Triomphe, B-1050 Brussels, Belgium, Ph.: 32-(0)2-650-5386, Fax: 32-(0)2-650-5382, email: vrauss@ulb.ac.be.

Short title: Structure of amyloid-β oligomers

Alzheimer's disease (AD) is linked to amyloid beta peptide (Aβ) misfolding. Studies demonstrate that the level of soluble Aβ oligomeric forms correlates better with the progression of the disease than the level of fibrillar forms. Conformation-dependent antibodies have been developed to detect either Aβ oligomers or fibrils, suggesting that structural differences between these forms of Aβ exist. Using conditions which yield well-defined Aβ(1-42) oligomers or fibrils, we studied the secondary structure of these species by attenuated total reflection-FTIR spectroscopy. Whereas fibrillar Aβ was organized in a parallel β-sheet conformation, oligomeric Aβ displayed distinct spectral features, which were attributed to an anti-parallel β-sheet structure. We also noted striking similarities between Aβ oligomers spectra and those of bacterial outer membrane porins. We discuss our results in terms of a possible organization of the anti-parallel β-sheets in Aβ oligomers, which may be related to reported effects of these highly toxic species in the amyloid pathogenesis associated with AD.

Alzheimer's disease (AD) is a widespread form of dementia belonging to the large family of amyloidoses whose common feature is the aggregation of misfolded proteins and/or peptides. AD is a brain-specific degenerative disease neuropathologically characterized by the presence of fibrillar amyloid deposition in extraneuronal spaces/cerebrovascular regions and by neurofibrillary tangles inside the neurons [1].

Amyloid plaques are primarily composed of amyloid-β (Aβ) peptide (38 to 43 residue long), which is released after proteolytic cleavage of the amyloid precursor protein (APP) by β- and γ-secretases [2]. The amyloid hypothesis suggests that Aβ accumulation in the brain is the primary event in the pathogenesis. Formation of tau tangles could be one of the consequences of an imbalance between production and clearance of Aβ [1]. Aβ(1-42) and Aβ(1-40) are the principal components of amyloid plaques [3]. Aβ(1-42) is the highly amyloidogenic though less abundant form, which appears to be initially deposited [4]. This higher ability of Aβ(1-42) to aggregate has been related to the two additional hydrophobic amino acids at its C-terminal end [5].

Several aggregation states have been identified for amyloidogenic proteins. Aβ can exist as a monomer or larger soluble entities called oligomers and eventually insoluble fibrils. The general term "oligomers" includes different kinds of assemblies such as dimers, trimers, protofibrils, Aβ-derived diffusible ligands (ADDLs), annular or pore-like oligomers [6]. Recently, it has also been reported that oligomers could be classified into prefibrillar or fibrillar oligomers as they have different aggregation pathways [7].

Aβ deposition in brain to form fibrillar plaques has been associated for a long time with neurodegeneration, insidious memory loss and cognitive decline [2, 8]. However, there has been a paradigm shift in this concept and it is now widely accepted that soluble oligomers of Aβ are more neurotoxic than Aβ fibrils and play a direct role in the amyloid pathogenesis [9]. Cognitive decline associated with AD precedes amyloid deposition in human and transgenic mouse models and correlates with soluble Aβ oligomers level rather than APP level or fibrillar amyloid deposits [10].

Aβ oligomers are most probably intermediates in the amyloid fibril formation. However, they are not necessarily required to form fibrils [11]. Recently, a conformation-dependent antibody has been shown to detect amyloid fibrils with high specificity, regardless of their sequence [7]. Previously, using another conformation-dependent antibody raised against Aβ prefibrillar oligomers, it was demonstrated that many amyloidogenic proteins or peptides, which also form oligomers, were recognized by the same antibody. Therefore, different types of amyloid oligomers may adopt a common structural motif postulated to be crucial in their common toxicity [12].

Thus, obtaining any new structural information about Aβ oligomers would be an important step in a better understanding of AD etiology and possibly other amyloidogenic diseases. Previous studies carried out on Aβ oligomers reported the dominance of β-sheet structures. However, they were unable to distinguish between parallel and anti-parallel structures. In this study, we use attenuated total reflection-Fourier transform infrared (ATR-FTIR) spectroscopy to compare the structure of Aβ(1-42) oligomers and fibrils. We demonstrate that although both forms adopt a predominantly β-sheet structure, Aβ(1-42) oligomers adopt an anti-parallel β-sheet structure, which is distinctly absent in fibrils.

EXPERIMENTAL

Peptide preparation. Aβ(1-42) was purchased from American Peptide Co. (Sunnyvale, CA). The peptide was dissolved in cold hexafluoroisopropanol (HFIP, Sigma-Aldrich, St. Louis, MO) at a 2 mg/ml concentration, incubated at room temperature for one hour and then aliquoted. HFIP was evaporated under nitrogen flow and residual HFIP removed under vacuum using a Speed Vac. The resulting Aβ(1-42) film was stored at –20°C until further manipulation.

Aβ(1-42) incubations. Prior to any incubation, the peptide was dissolved in dimethylsulfoxide (DMSO, Sigma-Aldrich, St. Louis, MO) at a final concentration of 5 mM and then immediately resuspended using one of the following conditions. To obtain oligomers, the peptide was either dissolved in F12 phenol red-free cell culture medium (Sigma-Aldrich, St. Louis, MO) as developed in Dahlgren et al. [13] and Stine et al. [14] or in 20 mM Tris-HCl, pH 7.4, 100 mM NaCl (Tris-buffered saline, TBS) as developed by Garzon-Rodriguez et al. [15], at a final concentration of 100 µM and incubated at 4°C for 24 h. To obtain fibrils, the peptide was resuspended either in 10 mM HCl at a final concentration of 100 µM and incubated at 37°C for 24 h, or in 0.5 mM Hepes pH 7.4 at a final concentration of 500 µM and incubated at room temperature under gentle agitation for at least 30 days.

Western blot analysis. Peptide samples were diluted in SDS-PAGE sample buffer and separated on a 12% bis-Tris gel at 4°C for 2 h at 100 V. The separated bands were transferred onto a nitrocellulose membrane which was then blocked for 1 h in 5% nonfat dry milk in TBS/Tween 20 buffer. The membrane was incubated with the mouse monoclonal Aβ antibody 6E10 (1:3000) (Sigma-Aldrich, St. Louis, MO). Detection was carried out using horseradish peroxidase-conjugated anti-mouse antibody (1:2000) and the Supersignal West Pico Chemiluminescent Substrate (Pierce Biotechnology, Rockford, IL). Pictures were recorded and analyzed using the ImageQuant 400 gel imager and ImageQuant TL software (GE Healthcare).

Atomic Force Microscopy. Aβ(1-42) solutions were characterized by atomic force microscopy (AFM) using a Nanoscope IIIa (Veeco Metrology LLC, Santa Barbara, CA) equipped with a 120 x 120 µm piezoelectric scanner. Analyses were carried out either in contact or in tapping mode at room temperature in air using AFM cantilevers with spring constant of either 0.01 or 0.03 N/m (Microlevers, Veeco Metrology LLC, Santa Barbara, CA). Before analysis, 100 µL of sample (diluted 10x in the case of fibrils and 5x in the case of oligomers) were incubated 10 min at room temperature on freshly cleaved mica and rinsed four times with milliQ water. Excess water was then removed under nitrogen flow.

Thioflavine T fluorescence. Thioflavine T (ThT, Sigma-Aldrich, St. Louis, MO) fluorescence was used to characterize the different peptide solutions according to LeVine [16] on a LS55 fluorimeter (Perkin Elmer Instruments). Briefly, 4.5 µg of peptide were added to 1 ml of a 5 µM ThT solution maintained at 25°C by a circulating water bath and the fluorescence was recorded at 482 nm (excitation wavelength: 450 nm).

Dot blot analysis. 1 µg of oligomeric Aβ was spotted onto a nitrocellulose membrane, which was subsequently blocked with 10% nonfat milk in TBS-0.01% Tween 20 for 1 h at 4°C and washed. Then the membrane was incubated overnight at 4°C with rabbit anti-oligomer antibody A11 (1:3000) in 5% nonfat milk TBS-0.01% Tween 20. After washing with TBS-0.01% Tween 20, the membrane was incubated for 1 h at 4°C with horseradish peroxidase-conjugated anti-rabbit IgG (Cell signaling technology, Danvers, MA) (1:2000). ECL western blot detection

system (GE Healthcare, Piscataway, NJ) was used to detect chemiluminescence and pictures were recorded and analyzed using the ImageQuant 400 gel imager and ImageQuant TL software (GE Healthcare).

IR spectroscopy. IR spectra were recorded on an Equinox 55 infrared spectrophotometer (Bruker Optics, Ettlingen, Germany) equipped with a Golden gate reflectance accessory (Specac, Orpington, U.K.). The internal reflection element was a diamond crystal (2 x 2 mm) with an aperture angle of 45° that yielded a single internal reflection. 128 accumulations were performed to improve the signal/noise ratio. The spectrometer was continuously purged with dried air. Spectra were recorded at a resolution of 2 cm^{-1}. All measurements were made at 24°C. Samples were prepared by spreading 2 µL of peptide solution on the diamond crystal surface and by removing the excess water under nitrogen flow. Alternatively, for salt-containing samples, similarly to the AFM sample preparation, 5 µL of peptide solution were incubated at the diamond surface for 15-20 min, the sample was then washed three times with excess milliQ water. Finally, excess water was removed under nitrogen flow.

H/D exchange. Hydrogen/deuterium (H/D) exchange experiments were performed on Aβ oligomers and fibrils. The pH of the samples was adjusted in order to perform the exchange on samples with identical pH. The decay of the NH-associated amide II band (1520-1580 cm^{-1}) was used to monitor the exchange of the amide group. Results were analyzed as previously described [17].

Spectral cluster analysis. Before analysis, a linear baseline was subtracted from all spectra at 1708, 1602, and 1482 cm^{-1}. Spectra were then rescaled on the amide I area (1708-1602 cm^{-1}). Spectra were clustered according to the Euclidian distances for each wavenumber in the amide I and II range (1708-1482 cm^{-1}).

Protein spectra used for the clustering analysis were extracted from the RASP50 database [18]: ADH Alcohol dehydrogenase from horse liver; ALA α-Lactalbumin from human milk; APE Apolipoprotein E3 from human; ATX α-Hemolysin (alphatoxin) from *Staphylococcus aureus;* AVI Avidin from hen egg white; BTE Erabutoxin b from *Laticauda semifasciata;* CAH Carbonic anhydrase from bovine erythrocyte; CNA Concanavalin A from jack bean; COL Colicin A, C-terminal domain from bacterial source; CSA Citrate synthetase from porcine heart; CTG α-Chymotrypsinogen A from bovine pancreas; CYC Cytochrome c from horse heart; DPR Dihydropteridine reductase from sheep liver; FTN Ferritin (apo) from horse spleen; GST Glutathione S-transferase from equine liver; HBN Hemoglobin from bovine blood; IGG Immunoglobulin γ from human; INS Insulin from bovine pancreas; LCL Lectin, lentil from lentil; LOX Lipoxygenase-1 from soybean; LSZ Lysozyme from chicken egg white; MBN Myoglobin from horse heart; MON Monellin from *Dioscoreophyllum cumminsii;* MTH Metallothionein II from rabbit liver; OVA Ovalbumin (egg albumin) from hen; PAB Parvalbumin from rabbit muscle; PAH Penicillin amidohydrolase from *Escherichia coli;* PAP Papain from papaya latex; PEP Pepsin from porcine stomach; PER Peroxidase from *Arthromyces ramosus;* PGK Phosphoglyceric kinase from baker's yeast; PGN Pepsinogen from pig stomach; PLA Phospholipase A2 from bovine pancreas; R61 DD-transpeptidase from *Streptomyces r61;* REN Rennin (chymosin b) from calf stomach; RIC Ricin from castor bean; RNA Ribonuclease A from bovine pancreas; SBC Subtilisin Carlsberg from *Bacillus licheniformus;* SBN Subtilisin BPN' (nagarse) from not specified; SDF Superoxide dismutase (Fe) from *Escherichia coli;* SOD Superoxide dismutase (Cu,Zn) from bovine erythrocyte; TGN Trypsinogen from bovine pancreas; TIB Trypsin inhibitor (soybean, Bowman-Burke) from soybean; TIP Trypsin inhibitor

(BPTI) from bovine pancreas; TMT Thaumatin from *Thaumatococcus daniellii;* TPI Triose phosphate isomerase from baker's yeast; TRO Troponin from chicken muscle; UBQ Ubiquitin from bovine erythrocyte; UOX Glucose oxidase from *Aspergillus niger;* XYN Xylanase from *Trichoderma viride* (see [18] for more details on the RASP50 FTIR database).

In addition to the RASP50 FTIR database spectra, spectrum from OmpF reconstituted in asolectin (kind gift from Dr. F. Homblé) and spectra of both Aβ(1-42) fibrils and oligomers (see Figures 2 and 3) were used.

RESULTS

Aβ(1-42) oligomers and fibrils: formation and assessments. Our goal in this study was to compare the structure of Aβ(1-42) oligomers and fibrils. We used well-defined oligomer- or fibril-forming protocols to obtain the desired Aβ(1-42) aggregates (see experimental section or references therein). Due to the inherent high structural variability of the peptide, we carefully assessed each species using four independent approaches to verify that we obtained the expected entities.

Since Aβ(1-42) is known to produce SDS-resistant oligomers and fibrils, we used bis-Tris SDS-PAGE followed by 6E10 monoclonal antibody recognition to visualize the different species. After incubation at 4°C for 24 h in TBS or F12, large oligomeric species appeared between ~40 and ~170 kDa (Figure 1, Panel A, lane 1). In acidic fibril-forming conditions, after 24 h of incubation, extremely high molecular weight Aβ remained in the stacking gel. This high molecular weight Aβ corresponded to fibrils. A decrease of tri- and tetrameric species was observed (Figure 1A, lane 2). For longer incubation time, in acidic fibril-forming conditions, the large oligomeric bands completely disappeared (Figure 1A, lane 3). Fibrils formed in 0.5 mM Hepes, pH 7.4 after 30 days also revealed an oligomer-free pattern (data not shown). It should be noted that the monomeric Aβ (~4.5 kDa) is present in all conditions. A quantification of the different band intensities using the ImageQuant TL software was carried out. It showed that in the oligomeric conditions (Figure 1A, lane 1), the band corresponding to the monomer represents only 16% of the total intensity while the larger oligomers (~40 to 170 kDa) represent 80% (trimers and tetramers represent 2% each). Such quantification is more difficult to perform for fibril-forming conditions because fibrils remain in the stacking gel and are most likely underestimated. Nevertheless, this result demonstrates that monomers are clearly not the major species in our samples. As a comparison, at t=0 in TBS, pH 7.4, Aβ(1-42) shows the presence of small oligomers (mainly trimers and tetramers) in addition to monomers which are the major species (~70%) presents on the Western Blot. High molecular weight oligomers are also present on a t=0 gel but do not represent a significant proportion (~3%) of the species formed by Aβ(1-42) (data not shown).

Even though Aβ is known to produce SDS-resistant oligomeric and/or fibrillar species, it has been shown that SDS-PAGE in the study of Aβ oligomers is not devoid of defects and might not always reflect the exact content of the different species present in the sample [6]. As suggested [6], we undertook further characterization of both oligomers and fibrils to ensure that our samples were representative of each species.

A second method used to confirm fibril or oligomer formation was AFM. AFM images of oligomers formed after 24 h showed the presence of globular spherical-shaped entities (Figure 1, Panel B, top) with a typical height of 5-6 nm, which is in good agreement with previously characterized oligomers [19]. Importantly, it also showed that no fibrils were present in our oligomer-forming conditions. This verification was critical for the subsequent IR analysis, since it excluded potential spectral contributions from fibrils. In fibril-forming conditions, AFM images showed long unbranched fibrils with a typical 7-8 nm width (Figure 1, Panel B, bottom). At higher magnification, these images showed some periodicity along the fibril axes (not shown). All these features are in agreement with previously published data on Aβ fibrils [20]. To ensure that these fibrils were not formed during AFM sample preparation, especially during the removal of excess water at the mica plate, fibrillar samples were observed in contact mode in

buffer. These fibrillar samples were prepared in HCl and then resuspended in TBS pH 7.4 to also ensure that a change in buffer and in pH do not affect the fibril morphology. The fibrils were not as well-resolved as in tapping mode in air. However, the overall morphology and the size of the fibrils resembled those in tapping mode (not shown), demonstrating that the removal of the excess water of the sample at the mica surface and a change in pH do not affect the fibrils once they are formed.

A third assessment was carried out using ThT fluorescence. ThT is known to fluoresce specifically in the presence of amyloid fibrils [16]. After resuspension (t=0h) of the Aβ(1-42) peptide in all the conditions used here, the samples are ThT negative. Both fibril-forming conditions resulted in a high ThT fluorescence emission intensity. This is already observed after 24h for fibrils formed in 10 mM HCl. On the other hand, all the oligomeric samples showed negligible ThT fluorescence emission intensity even after 48h (Figure 1, Panel C).

Finally, using A11, an oligomeric conformation-specific antibody [12], we demonstrated by dot blot analysis that oligomer-forming protocols yielded A11 positive results (Figure 1, Panel D, top for oligomers formed in TBS). Fibrils formed in 10 mM HCl responded poorly or weakly to A11 after one week incubation (Figure 1, Panel D, bottom).

Taken together, these four experiments independently confirm that the oligomeric preparations: (i) do not have any fibrillar species, and, (ii) do indeed contain moieties that are detected by the A11 antibody. Conversely, this analysis also ensures that our Aβ fibril samples are ThT positive and devoid of oligomers. This rigorous pre-analysis is essential in our subsequent FTIR analysis to ensure that our oligomeric Aβ species do not contain any fibrillar species (and vice versa) that may potentially contribute to the spectral signals.

Secondary structure of oligomeric and fibrillar Aβ(1-42) species. We then examined the secondary structure of these well-defined oligomeric and fibrillar Aβ(1-42) species by ATR-FTIR. In FTIR, it has been demonstrated both theoretically and experimentally that parallel and anti-parallel β-sheet structures can be distinguished based on the analysis of the amide I (1700-1600 cm^{-1}) region [21]. In anti-parallel β-sheet structures, the amide I region displays two typical components. The major component has an average wavenumber located at ~1630 cm^{-1} while the minor component, about five fold weaker than the major one, is characterized by an average wavenumber at 1695 cm^{-1}. The 1695/1630 intensity ratio has been suggested to be proportional to the percentage of anti-parallel arrangement of the β-strands in a β-sheet [22]. For parallel β-sheet structures, the amide I region displays only the major component around 1630 cm^{-1} [23, 24].

FTIR spectra of Aβ(1-42) in the two fibril-forming conditions employed in this study (Figure 2, spectra *a* and *b*) showed typical parallel β-sheet features, characterized by a maximum of absorbance at 1630 cm^{-1} in the amide I region. The relatively narrow width of the major peak at 1630 cm^{-1} is indicative of stable and/or long β-strands and strong hydrogen bonds [24], as expected for extremely stable structure like amyloid fibrils.

FTIR spectra of Aβ(1-42) oligomers were significantly different from those of Aβ(1-42) fibrils, indicating that these entities adopt a different structure. The amide I region is characterized by the presence of the two characteristic components of anti-parallel β-sheet structure, at 1630 and 1695 cm^{-1} (Figure 3, spectrum *a-c*).

A quantitative analysis of the amide I region by deconvolution followed by curve-fitting showed that for both Aβ(1-42) oligomers and fibrils, β-sheet structures were the most abundant

(48-57% and ~75% respectively), while random coil and/or helical structures (observed absorbance around 1650-1660 cm^{-1}) represented ~20-26 and ~5-10% for the oligomers and fibrils, respectively. The helical content was slightly higher (33% and ~40% if we take into account the random coil contribution) in oligomers incubated less than 1h, indicating a change in structure from α-helix to β-sheet, with time. β-turns content (~1670 cm^{-1}) was ~15-20% for all the structures studied here.

Solvent accessibility: hydrogen/deuterium exchange experiments. To further analyze the structural difference between Aβ(1-42) oligomers and fibrils, we performed hydrogen/deuterium exchange experiments using FTIR spectroscopy. While Aβ(1-42) oligomers showed relatively fast exchange dynamics (about 60% of amide hydrogens exchanged after one hour), Aβ(1-42) fibrils had a slower exchange dynamics (only ~40% of amide hydrogens exchanged during the same period of time) (Figure 4). The initial exchange rate was extremely rapid especially for oligomers where most of the exchange occurred during the first five minutes.

Comparison with other proteins. In order to compare the different structures produced here with known protein structures, we used a protein IR spectra database [18] designed to cover as well as possible the conformational space as defined by CATH [25], with almost no redundancies. This database was previously shown to contain a number of unique features and allowed an improved structure prediction from infrared spectra [26, 27].

The overall shape of the Aβ(1-42) spectra in the amide I and II range was compared with the entire database by mean of a cluster analysis based on Euclidian distance measurement (see materials and methods and Figure 5). The results demonstrated that (i) Aβ fibrils spectra do not cluster with other protein spectra and that (ii) Aβ oligomers spectra are clustered with 5 anti-parallel β-sheet proteins (namely avidin, concanavalin A, lentil lectin, OmpF, and xylanase). From this cluster analysis, it is clear that OmpF spectrum is the closest and most related to the Aβ oligomer ones (Figure 3, spectrum *d*, and Figure 5). OmpF is folded as a typical anti-parallel β-sheet barrel made of 16 anti-parallel strands and is associated with an almost 100% anti-parallel arrangement of its β-strands [28]. The spectrum reveals the presence of 1630 and 1695 cm^{-1} peaks, attributed to anti-parallel β-sheet structure. Using the respective 1695/1630 cm^{-1} intensity ratios [21] (Figure 6) for the different spectra displayed in Figure 2 and 3, we calculated that in all the oligomer-forming conditions used here, the percentage of anti-parallel arrangement of the β-strands was ~100%, while in fibril-forming conditions this percentage was lower than 10%.

DISCUSSION

The objective of our study was to investigate the secondary structure adopted by oligomeric Aβ in comparison with fibrillar Aβ, in an effort to understand the structural basis of the neurotoxicity associated with the former. While models for Aβ(1-40) and Aβ(1-42) in fibrillar conformations, mainly based on solid-state NMR data, are now accessible [29-32], almost no structural information for Aβ oligomers is currently available.

It is recognized that both species are characterized by the presence of β-sheet structures. However, fundamental differences in their local structures exist, confering them unique reactivity with conformation-specific antibodies. Using well-defined conditions, we prepared Aβ(1-42) oligomers and fibrils. The formation of Aβ oligomers or fibrils was confirmed with well-established tests that mutually complement each other, such as: (i) the presence of SDS-resistant entities of multiple molecular weights by SDS-PAGE, (ii) visualization of oligomeric and fibrillar species by AFM, (iii) confirmation of the absence of fibrils in our oligomer preparations and of the presence of fibrils in our fibril-forming conditions by ThT fluorescence, and (iv) verification of the presence of A11-reactive species in our oligomer preparations and not in our fibril preparations. This suite of assessments was critical for our subsequent FTIR analysis as it was important to demonstrate the absence of fibrillar Aβ in our oligomeric preparations and vice versa. As noted above, in the SDS-PAGE one intriguing point is the presence of monomeric Aβ in each lane. This monomeric band, which is clearly not the most abundant entity (see results), might be in part induced by the presence of SDS. If present in our samples, the monomers would contribute a constant spectral background in all our preparations.

After this initial confirmation, we employed ATR-FTIR to compare the structure of Aβ(1-42) oligomers and fibrils. In fibrils, the presence of a major narrow peak located at ~1630 cm^{-1} was indicative of a highly stable parallel β-sheet, in agreement with solid-state NMR models [29-32] and site-directed spin labeling experiments [33], which showed that both Aβ(1-40) and (1-42) adopt a cross-β structure with a parallel, in register, β-sheet composed of two strands connected by a turn or a loop region. Fifteen to twenty years ago, FTIR was first misleading and demonstrated that Aβ fibrils adopted an anti-parallel conformation. It is not our purpose here to discuss why such a discrepancy occurred in the past. More recently, several groups have demonstrated that for well-characterized parallel fibrils, the corresponding FTIR spectra were typical of parallel β-sheet (see for examples for Aβ(1-40), fig. 3d in [34], and for Aβ(1-28), fig. 2c in [35]). On the contrary, for well-characterized anti-parallel fibrils, FTIR spectra display two peaks (at ~1630 and ~1695 cm^{-1}) characteristic of anti-parallel β-sheet (see for example [36-38]).

A curve-fitting procedure of the infrared spectra revealed that the β-sheet content in fibrils was as high as ~75%. Solvent accessibility evaluated by NMR approach, indicated that there are two regions in Aβ(1-42) fibrils protected from the solvent. These two regions encompass 70% of the amino acids and are responsible for the formation of two strands in fibrils [39]. Using hydrogen/deuterium exchange, we showed that ~60% of the amide bonds of the peptide were protected against the exchange in the fibril conformation, which is also in very good agreement with data provided by deuterium exchange monitored by mass spectrometry [40].

It is believed that immediately upon its release from the membrane Aβ oligomerizes in dimers and other multimers or soluble oligomers, and possibly forms fibrils. Also referred to as protofibrils or ADDLs, soluble oligomers mediate neuronal toxicity, inhibit long-term potentiation [41] and modulate neuronal viability [6, 9], reflecting their inherent toxicity.

Oligomers formed in F12 cell culture medium, using the same protocol as we used here, have been tested for their toxicity on Neuro-2A neuroblastoma cells [13]. The authors showed that Aβ(1-42) oligomers inhibited neuronal viability 10 times more than Aβ(1-42) fibrils. Using the same conditions, the same group has tested the toxicity of Aβ(1-42) oligomers on neurons using primary co-cultures of neurons and glial cells [42]. They demonstrated that oligomeric Aβ(1-42) but not fibrillar Aβ(1-42) induced a dose-dependent increase in neurotoxicity. Thus, the related toxicity of the Aβ(1-42) oligomers we formed here, has been carefully tested. Unfortunately little structural information is currently available on oligomers. Nevertheless hydrogen-deuterium exchange on Aβ(1-40) protofibrils, which collectively referred to nonfibrillar oligomeric forms of Aβ, has shown that about 40% of the amide backbone are highly resistant to exchange [40]. This is in excellent agreement with the percentage we determined here on Aβ(1-42) oligomers. This also establishes the validity of the approach we employed to assess the oligomeric species. The β-sheet content in oligomers was lower than in fibrils but however significant and reached 48-57%. This lower content in secondary structure and faster exchange dynamics probably reflect a higher flexibility of Aβ in soluble oligomers than in fibrils. This higher flexibility (or lower stability) may be a crucial property of such assemblies, especially in their mechanism of toxicity. One of the hypothetical toxicity mechanisms for oligomers is related to their interaction with lipid bilayers in which they might cause perturbation and/or permeabilization [43-45].

Compared to fibrils, infrared spectra of oligomers revealed the presence of an additional peak located at 1695 cm^{-1}, indicative of an anti-parallel β-sheet conformation in these species. This additional peak has been recently observed in Aβ(1-40) oligomers [34] and also in oligomers formed by a prion peptide (PrP82-146) [46]. This structural information suggests that even if fibrils and oligomers are rich in β-sheets, they do not adopt the same conformation. This is of significance in the neurotoxicity associated with oligomers. The anti-parallel β-sheet organization in oligomers might represent a critical step in perturbation and/or permeabilization of biological membranes [43-45].

The A11 oligomer-specific antibody does not recognize fibrils or low molecular weight oligomers but is able to recognize higher molecular weight prefibrillar oligomers of a wide variety of amyloidogenic peptides or proteins [12]. This suggests that most, if not all, amyloidogenic oligomers adopt the same structure and might share the same mechanism of toxicity. Recently, the same antibody was used with success against the pore-forming bacterial toxin, α-hemolysin, and on human perforin [47]. These proteins are known to form oligomeric pores in their toxic conformation, each monomer supplying several β-strands which self-assemble to fold into a β-barrel. It has been shown that Aβ and other amyloids can form annular or ring-shaped particles [44] which are comparable to pore-forming proteins.

Infrared spectra of Aβ oligomers presented striking similarities with bacterial outer membrane porins, which are folded as β-barrels. Based on the 1695/1630 cm^{-1} intensity ratios, we determined that Aβ oligomers were composed of β-strands, all of which were in an anti-parallel organization. Interestingly, all pore-forming β-barrels adopt an anti-parallel β-sheet organization. Based on the secondary structure content (45-50% of extended β-sheet structures), we postulate a putative model wherein each Aβ molecule will provide two β-strands upon self-assembling during oligomer formation. In our view, the simplest way to accommodate two β-strands into the Aβ peptide in oligomeric conformation is to postulate that the two strands present in fibrils and encompassing approximately residues ~11-24 and ~28-42 [32], will form

shorter β-strands in oligomers encompassing about 10 to 12 residues each. These strands self-assemble in an anti-parallel β-sheet conformation (Figure 3, 5, and 7). Recently, the structure of monomeric Aβ(1-40) in complex with a phage-display selected affibody protein has been solved by NMR spectroscopy [49]. This structure clearly showed that monomeric Aβ(1-40) when stabilized by neighbor structural elements can adopt an anti-parallel β hairpin involving two β-strands encompassing residues 17-23 and 30-36. This is in good agreement with our proposed anti-parallel β-sheet model. As suggested by Hoyer and coworkers [49], it can be speculated that in our proposed model, a "simple" reorientation of the plane of the strands by 90° will allow a reorganization from an anti-parallel to a parallel β-sheet conformation, a conformational change that may be associated with the conversion from oligomeric to fibrillar Aβ and vice versa. Further, it can be suggested that the anti-parallel β-sheet conformation of oligomeric Aβ(1-42) might in some case(s) be the early stages in the formation of a β-barrel made of amphipathic strands, 10-12 residue long each. This β-barrel conformation (see figure 7 for a schematic representation) is ideally suited to insert into a cellular membrane and span a lipid bilayer. Such an organization can potentially lead to permeabilization of cells, thereby contributing to the toxicity associated with these species. We suggest that, in the anti-parallel conformation, the β-strands are organized in a manner that allows intra-molecular hydrogen bond formation, and not only inter-molecular ones like in fibrils.

In conclusion, we demonstrated using ATR-FTIR spectroscopy that: (i) Aβ(1-42) oligomers and fibrils can be clearly distinguished from each other and do not adopt the same secondary and tertiary structure, and (ii) Aβ(1-42) oligomers adopt an anti-parallel β-sheet conformation. The anti-parallel β-sheet structure may thus be a signature structural feature of oligomeric Aβ. (iii) We showed some striking spectral similarities between Aβ oligomers and pore-forming porins and therefore believe that the ability of Aβ oligomers to form a porin-like structure may be associated with their toxicity in AD.

REFERENCES

1. Hardy, J. and Selkoe, D.J. (2002) The amyloid hypothesis of Alzheimer's disease: progress and problems on the road to therapeutics. Science **297**, 353-356.
2. Selkoe, D.J. (1998) The cell biology of beta-amyloid precursor protein and presenilin in Alzheimer's disease. Trends Cell. Biol. **8**, 447-453.
3. Vigo-Pelfrey, C., Lee, D., Keim, P., Lieberburg, I. and Schenk, D.B. (1993) Characterization of beta-amyloid peptide from human cerebrospinal fluid. J. Neurochem. **61**, 1965-1968.
4. Jarrett, J.T., Berger, E.P. and Lansbury, P.T.Jr. (1993) The carboxy terminus of the beta amyloid protein is critical for the seeding of amyloid formation: implications for the pathogenesis of Alzheimer's disease. Biochemistry **32**, 4693-4697.
5. Kim, W. and Hecht, M.H. (2005) Sequence determinants of enhanced amyloidogenicity of Alzheimer A{beta}42 peptide relative to A{beta}40. J. Biol. Chem. **280**, 35069-35076.
6. Bitan, G., Fradinger, E.A., Spring, S.M. and Teplow, D.B. (2005) Neurotoxic protein oligomers--what you see is not always what you get. Amyloid **12**, 88-95.
7. Kayed, R., Head, E., Sarsoza, F., Saing, T., Cotman, C.W., Necula, M., Margol, L., Wu, J., Breydo, L., Thompson, J.L., Rasool, S., Gurlo, T., Butler, P. and Glabe, C.G. (2007) Fibril specific, conformation dependent antibodies recognize a generic epitope common to amyloid fibrils and fibrillar oligomers that is absent in prefibrillar oligomers. Mol. Neurodegener. **2**, 18-28.
8. Selkoe, D.J. (1996) Amyloid β-Protein and the Genetics of Alzheimer's Disease. J. Biol. Chem. **271**, 18295-18298.
9. Kirkitadze, M.D., Bitan, G. and Teplow, D.B. (2002) Paradigm shifts in Alzheimer's disease and other neurodegenerative disorders: the emerging role of oligomeric assemblies. J. Neurosci. Res. **69**, 567-577.
10. Mucke, L., Masliah, E., Yu, G.Q., Mallory, M., Rockenstein, E.M., Tatsuno, G., Hu, K., Kholodenko, D., Johnson-Wood, K. and McConlogue, L. (2000) High-level neuronal expression of abeta 1-42 in wild-type human amyloid protein precursor transgenic mice: synaptotoxicity without plaque formation. J. Neurosci. **20**, 4050-4058.
11. Necula, M., Kayed, R., Milton, S. and Glabe C.G. (2007) Small molecule inhibitors of aggregation indicate that amyloid beta oligomerization and fibrillization pathways are independent and distinct. J. Biol. Chem. **282**, 10311–10324.
12. Kayed, R., Head, E., Thompson, J.L., McIntire, T.M., Milton, S.C., Cotman, C.W. and Glabe, C.G. (2003) Common structure of soluble amyloid oligomers implies common mechanism of pathogenesis. Science **300**, 486-489.
13. Dahlgren, K.N., Manelli, A.M., Stine, W.B. Jr, Baker, L.K., Krafft, G.A., LaDu, M.J.. (2002) Oligomeric and fibrillar species of amyloid-beta peptides differentially affect neuronal viability. J Biol Chem. **277**, 32046-32053.

14. Stine, W.B. Jr, Dahlgren, K.N., Krafft, G.A., LaDu, M.J.. (2003) In vitro characterization of conditions for amyloid-beta peptide oligomerization and fibrillogenesis. J Biol Chem. **278**, 11612-11622.

15. Garzon-Rodriguez, W., Sepulveda-Becerra, M., Milton, S.C. and Glabe, C.G. (1997) Soluble amyloid Abeta-(1-40) exists as a stable dimer at low concentrations. J. Biol. Chem. **272**, 21037-21044.

16. LeVine, H. III (1999) Quantification of beta-sheet amyloid fibril structures with thioflavin T. Meth. Enzymol. **309**, 274-284.

17. Goormaghtigh, E., Raussens, V. and Ruysschaert, J-M. (1999) Attenuated total reflection infrared spectroscopy of proteins and lipids in biological membranes. Biochim Biophys Acta. **1422**, 105-185.

18. Oberg, K.A., Ruysschaert, J.M. and Goormaghtigh, E. (2003) Rationally selected basis proteins: a new approach to selecting proteins for spectroscopic secondary structure analysis. Protein Sci. **12**, 2015-2031.

19. Mastrangelo, I.A., Ahmed, M., Sato, T., Liu, W., Wang, C., Hough, P. and Smith, S.O. (2006) High-resolution atomic force microscopy of soluble Abeta42 oligomers. J. Mol. Biol. **358**, 106-119.

20. Stromer, T. and Serpell, L.C. (2005) Structure and morphology of the Alzheimer's amyloid fibril. Microsc Res Tech. **67**, 210-217.

21. Miyazawa, T. and Blout, E.R. (1961) The infrared spectra of polypeptides in various conformations: Amide I and Amide II bands J. Am. Chem. Soc. **83**, 712-719.

22. Chirgadze, Y.N. and Nevskaya, N.A. (1976) Infrared Spectra and resonance Interaction of Amide-I Vibration of the Antiparallel-Chain Pleated Sheet. Biopolymers **15**, 607-625.

23. Chirgadze, Y.N. and Nevskaya, N.A. (1976) Infrared Spectra and resonance Interaction of Amide-I Vibration of the Parallel-Chain Pleated Sheet. Biopolymers **15**, 627-636.

24. Goormaghtigh, E., Cabiaux, V. and Ruysschaert, J-M. (1994) Determination of soluble and membrane protein structure by Fourier transform infrared spectroscopy. I. Assignments and model compounds. Subcell. Biochem. **23**, 329-362.

25. Orengo, C.A., Michie, A.D., Jones, S., Jones, D.T., Swindells, M.B. and Thornton, J.M. (1997) CATH--a hierarchic classification of protein domain structures. Structure **5**, 1093-1108.

26. Oberg, K.A., Ruysschaert J.-M. and Goormaghtigh, E. (2004) The optimization of protein secondary structure determination with infrared and circular dichroism spectra. Eur.J.Biochem. **271**, 2937-2948.

27. Goormaghtigh,E., Ruysschaert, J.-M. and Raussens, V. (2006) Evaluation of the information content in infrared spectra for protein secondary structure determination. Biophys. J. **90**, 2946-2957.

28. Cowan, S.W., Schirmer, T., Rummel, G., Steiert, M., Ghosh, R., Pauptit, R.A., Jansonius, J.N. and Rosenbusch, J.P. (1992) Crystal structures explain functional properties of two E. coli porins. Nature **358**, 727-733.

29. Antzutkin, O.N., Balbach, J.J., Leapman, R.D., Rizzo, N.W., Reed, J. and Tycko, R. (2000) Multiple quantum solid-state NMR indicates a parallel, not antiparallel, organization of

beta-sheets in Alzheimer's beta-amyloid fibrils. Proc. Natl. Acad. Sci. USA **97**, 13045-13050.

30. Petkova, A.T., Ishii, Y., Balbach, J.J., Antzutkin, O.N., Leapman, R.D., Delaglio, F. and Tycko, R. (2002) A structural model for Alzheimer's beta -amyloid fibrils based on experimental constraints from solid state NMR. Proc. Natl. Acad. Sci. USA **99**, 16742-16747.
31. Petkova, A.T., Yau, W-M. and Tycko, R. (2006) Experimental constraints on quaternary structure in Alzheimer's beta-amyloid fibrils. Biochemistry **45**, 498-512.
32. Lührs, T., Ritter, C., Adrian, M., Riek-Loher, D., Bohrmann, B., Döbeli, H., Schubert, D. and Riek, R. (2005) 3D structure of Alzheimer's amyloid-beta(1-42) fibrils. Proc. Natl. Acad. Sci. U.S.A **102**, 17342-17347.
33. Török, M., Milton, S., Kayed, R., Wu, P., McIntire, T., Glabe, C.G. and Langen, R. (2002) Structural and dynamic features of Alzheimer's Abeta peptide in amyloid fibrils studied by site-directed spin labeling. J. Biol. Chem. **277**, 40810-40815.
34. Habicht, G., Haupt, C., Friedrich, R.P., Horstchansky, P., Sachse, C., Meinhardt J., Wieligmann, K., Gellerman, G.P., Brodhun, M., Götz, J., Halbhuber, K.-J., Röcken, C., Horn, U., Fändrich, M. (2007) Directed selection of a conformational antibody domain that prevents mature amyloid fibril formation by stabilizing Aβ protofibrils. Proc. Natl. Acad. Sci., USA **104**, 19232-19237.
35. Perálvarez-Marín, A., Barth, A., Gräslund, A. (2008) Time-Resolved Infrared Spectroscopy of pH-Induced Aggregation of the Alzheimer Aβ1–28 Peptide. J. Mol. Biol. **379**, 589–596.
36. Dzwolak and Smirnovas (2005) A conformational α-helix to β-sheet transition accompanies racemic self-assembly of polylysine: an FT-IR spectroscopic study. Biophys. Chem. **115**, 49-54
37. Castelletto, V., Hamley, I.W., Harris, P.J.F. (2008) Self-assembly in aqueous solution of a modified amyloid beta peptide fragment. Biophys. Chem. **138**, 29-35
38. Lee, S.-W., Mou, Y., Lin, S.-Y., Chou, F.-C., Tseng, W.H., Chen, C.-H., Lu C.-Y.D., Yu, S.S.-F., Chan, J.C.C. (2008) Steric Zipper of the Amyloid Fibrils Formed by Residues 109–122 of the Syrian Hamster Prion Protein. J. Mol. Biol. **378**, 1142-1154
39. Olofsson, A., Sauer-Eriksson, A.E. and Öhman, A. (2006) The solvent protection of alzheimer amyloid-beta-(1-42) fibrils as determined by solution NMR spectroscopy. J. Biol. Chem. **281**, 477-483.
40. Kheterpal, I., Lashuel, H.A., Hartley, D.M., Waltz, T., Lansbury, P.T. and Wetzel, R. (2003) Abeta protofibrils possess a stable core structure resistant to hydrogen exchange. Biochemistry **42**, 14092-14098.
41. Walsh, D.M., Klyubin, I., Fadeeva, J.V., Cullen, W.K., Anwyl, R., Wolfe, M.S., Rowan, M.J. and Selkoe, D.J. (2002) Naturally secreted oligomers of amyloid beta protein potently inhibit hippocampal long-term potentiation in vivo. Nature **416**, 535-539.
42. Manelli A.M., Bulfinch L.C., Sullivan P.M., LaDu M.J. (2007) Aβ42 neurotoxicity in primary co-cultures: Effect of apoE isoform and Aβ conformation. Neurobiol. Aging **28**, 1139-1147.

43. Kayed, R., Sokolov, Y., Edmonds, B., McIntire, T.M., Milton, S.C., Hall, J.E. and Glabe C.G. (2004) Permeabilization of lipid bilayers is a common conformation-dependent activity of soluble amyloid oligomers in protein misfolding diseases. J. Biol. Chem. **279**, 46363-46366.

44. Lashuel, H.A., Hartley, D., Petre, B.M., Walz, T. and Lansbury, P.T.Jr. (2002) Neurodegenerative disease: amyloid pores from pathogenic mutations. Nature **418**, 291.

45. Kremer, J.J., Pallitto, M.M., Sklansky, D.J. and Murphy, R.M. (2000) Correlation of beta-amyloid aggregate size and hydrophobicity with decreased bilayer fluidity of model membranes. Biochemistry **39**, 10309-10318.

46. Natalello, A., Prokorov, V.V., Tagliavini, F., Morbin, M., Forloni, G., Beeg, M., Manzoni, C., Colombo, L., Gobbi, M., Salmona, M., Doglia, S.M. (2008) Conformational plasticity of the Gerstmann-Sträussler-Scheinker disease peptide as indicated by its multiple aggregation pathways. J. Mol. Biol. **381**, 1349-1361.

47. Yoshiike, Y., Kayed, R., Milton, S.C., Takashima, A. and Glabe, C.G. (2007) Pore-forming proteins share structural and functional homology with amyloid oligomers. Neuromolecular Med. **9**, 270-275.

48. Tomaselli, S., Esposito, V., Vangone, P., van Nuland, N.A., Bonvin, A.M., Guerrini, R., Tancredi, T., Temussi, P.A. and Picone D. (2006) The alpha-to-beta conformational transition of Alzheimer's Abeta-(1-42) peptide in aqueous media is reversible: a step by step conformational analysis suggests the location of beta conformation seeding. Chembiochem. **7**, 257-267.

49. Hoyer, W., Grönwall, C., Jonsson, A., Ståhl, S., and Härd, T. (2008) Stabilization of a beta-hairpin in monomeric Alzheimer's amyloid-beta peptide inhibits amyloid formation. Proc. Natl. Acad. Sci. USA **105**, 5099-5104.

FOOTNOTES

Acknowledgment. The authors thank Drs. Cédric Govaerts and Fabrice Homblé for insightful discussions, Dr. Charles G. Glabe for kindly providing the A11 conformational-dependant antibody, Dr. F. Homblé for providing the OmpF porin FTIR spectrum and Drs. P. Boussard and Y. Looze for assistance and access to the fluorimeter. E.C. is Research Fellow for the National Fund for Scientific Research (Belgium), R.S. is Research Fellow for the Fund for Research in the Industry and Agriculture (Belgium), Y.D, V.R. are Senior Research Associate, and E.G is Research Director for the National Fund for Scientific Research (Belgium). V.N. was supported by funds from the Grant-In-Aid from the American Heart Association, the Drake Family trust and TRDRP. S.T.K is supported by a fellowship from the American Heart Association.

The abbreviations used are: Aβ, amyloid-beta, AD, Alzheimer's disease, ADDLs, Aβ-derived diffusible ligands, AFM, atomic force microscopy, APP, amyloid precursor protein, ATR, attenuated total reflection, DMSO, dimethylsulfoxide, FTIR, Fourier transform infrared spectroscopy, HFIP, hexafluoroisopropanol, TBS, Tris-buffered saline solution, ThT, thioflavine T.

Keywords: Amyloid-beta, Alzheimer's disease, oligomeric Abeta, anti-parallel beta-sheet, OmpF, secondary structure, infrared spectroscopy.

FIGURE LEGENDS

Figure 1. Assessments of Aβ(1-42) in oligomer- and fibril-forming conditions. A. Western blot analysis of Aβ(1-42) oligomers and fibrils separated on a 12% bis-Tris SDS-PAGE and probed with the monoclonal antibody 6E10. Lane 1 shows Aβ(1-42) oligomers formed in TBS after 24 h. Lanes 2 and 3 show Aβ(1-42) fibrils formed in 10 mM HCl after 24 h and 7 days, respectively. A quantification on non-overexposed blots has been carried out using the ImageQuant gel imager and software (see text). **B**. AFM images of oligomeric and fibrillar Aβ(1-42). AFM images were recorded in 2 x 2 μm contact mode with oligomers formed in TBS after 24 h (total z range = 15 nm) (top) and 2 x 2 μm tapping mode with fibrils formed in 10 mM HCl after 24 h (total z range = 8 nm) (bottom). **C**. Relative ThT fluorescence emission intensity after 0, 24, and 48 h for Aβ(1-42) oligomers formed in TBS (black), in F12 medium (light grey), and for Aβ(1-42) fibrils formed in 10 mM HCl (dark grey). **D**. Dot blot analysis of 1 μg of Aβ(1-42) oligomers formed in TBS after 24h (top) and fibrils formed in 10 mM HCl after 1 week (bottom) with the conformation-dependent A11 antibody. The results shown here are representative from 3-5 independent experiments.

Figure 2. ATR-FTIR spectra in the amide I region of Aβ(1-42) in fibril-forming conditions. a, Aβ(1-42) fibrils formed in 0.5 mM Hepes, pH 7.4 under agitation for 36 days. **b**, Aβ(1-42) fibrils formed in 10 mM HCl during 7 days. Spectral intensities were normalized to the intensity of the 1630 cm^{-1} peaks. Spectra were shifted for better visualization. Spectra were deconvoluted using a Lorentzian deconvolution factor with a full width at half height of 20 cm^{-1}, a Gaussian apodization factor with a full width at half height of 13.33 cm^{-1} to obtain a resolution enhancement factor K = 1.5 [24]. Spectra are representative of at least 3 independent experiments.

Figure 3. ATR-FTIR spectra in the amide I region of Aβ(1-42) in oligomer-forming conditions. a and **b**, Aβ(1-42) oligomers after incubation in TBS for < 1 h and 24 h, respectively. **c**, Aβ(1-42) oligomers formed in F12 cell culture medium after 24 h. **d**, bacterial porin OmpF reconstituted in lipid membrane. Spectral intensities were normalized to the intensity of the 1630 cm^{-1} peaks. Spectra were shifted for better visualization. All spectra were deconvoluted using a Lorentzian deconvolution factor with a full width at half height of 20 cm^{-1}, a Gaussian apodization factor with a full width at half height of 13.33 cm^{-1} to obtain a resolution enhancement factor K = 1.5 [24]. Vertical dashed line was added at 1695 cm^{-1} to facilitate the identification of differences between spectra. Spectra are representative of at least 3 independent experiments.

Figure 4. Hydrogen/deuterium exchange of Aβ(1-42) fibrils (circles) and oligomers (triangles) as a function of time. Fibrils were formed in 10 mM HCl and oligomers in TBS. Before experiments, pH for both samples was adjusted to 6.5. Data are representative of at least 3 independent experiments. Standard deviations between 3 experiments are ≤ 5%.

Figure 5. Dendrogram of the cluster analysis of RASP50, OmpF, Aβ(1-42) fibril and oligomer spectra in the amide I and II range (1708-1482 cm^{-1}). Abscissa is the Euclidean distance between spectra. On the ordinate the protein spectra identification are displayed. The

proteins corresponding to the three letters code for RASP50 proteins are listed above. Ompf.ir corresponds to the FTIR spectrum of bacterial OmpF. Fibrils_low_salt.ir corresponds to Aβ(1-42) fibrils formed in low salt condition; fibrils_HCl.ir corresponds to Aβ(1-42) fibrils formed in acidic condition. Oligos_TBS_0h.ir corresponds to Aβ(1-42) oligomers formed in TBS (t < 1h); oligosTBS_24h.ir corresponds to Aβ(1-42) oligomers formed in TBS (t = 24h); oligosF12_24h.ir corresponds to Aβ(1-42) formed in F12 cell culture medium (t = 24h).

Figure 6. Relative intensity ratios of the 1695 and 1630 cm^{-1} peaks for Aβ(1-42) fibrils and oligomers. a, for Aβ(1-42) fibrils formed in 0.5 mM Hepes, pH 7.4 under agitation for 30 days. **b**, for Aβ(1-42) fibrils formed in 10 mM HCl during 1 week, **c**, Aβ(1-42) oligomers after incubation in TBS for 24 h. **d**, Aβ(1-42) oligomers formed in F12 cell culture medium after 24 h. **e**, bacterial porin OmpF reconstituted in lipid membrane. All the 1695/1630 cm^{-1} ratios have been normalized on the OmpF ratio (taken as 100%). Inset: corresponding FTIR spectra in the 1695 cm^{-1} region.

Figure 7. A hypothetical schematic representation of Aβ oligomers in a putative pore-forming conformation. The monomer structure of Aβ was taken from the 1Z0Q PDB file [48], fibril structure was derived from the 2BEG PDB file [29]. The size of the pore and the number of strands involved in pore formation are hypothetical. Residues involved in the central strand region are colored in magenta; those in the C-terminal portion of Aβ peptide are in cyan. Non-structured regions are represented in green. The N-terminal region of the peptide is only represented in the monomer structure. The figure was made using Pymol.

Biochemical Journal Immediate Publication. Published on 13 May 2009 as manuscript BJ20090379

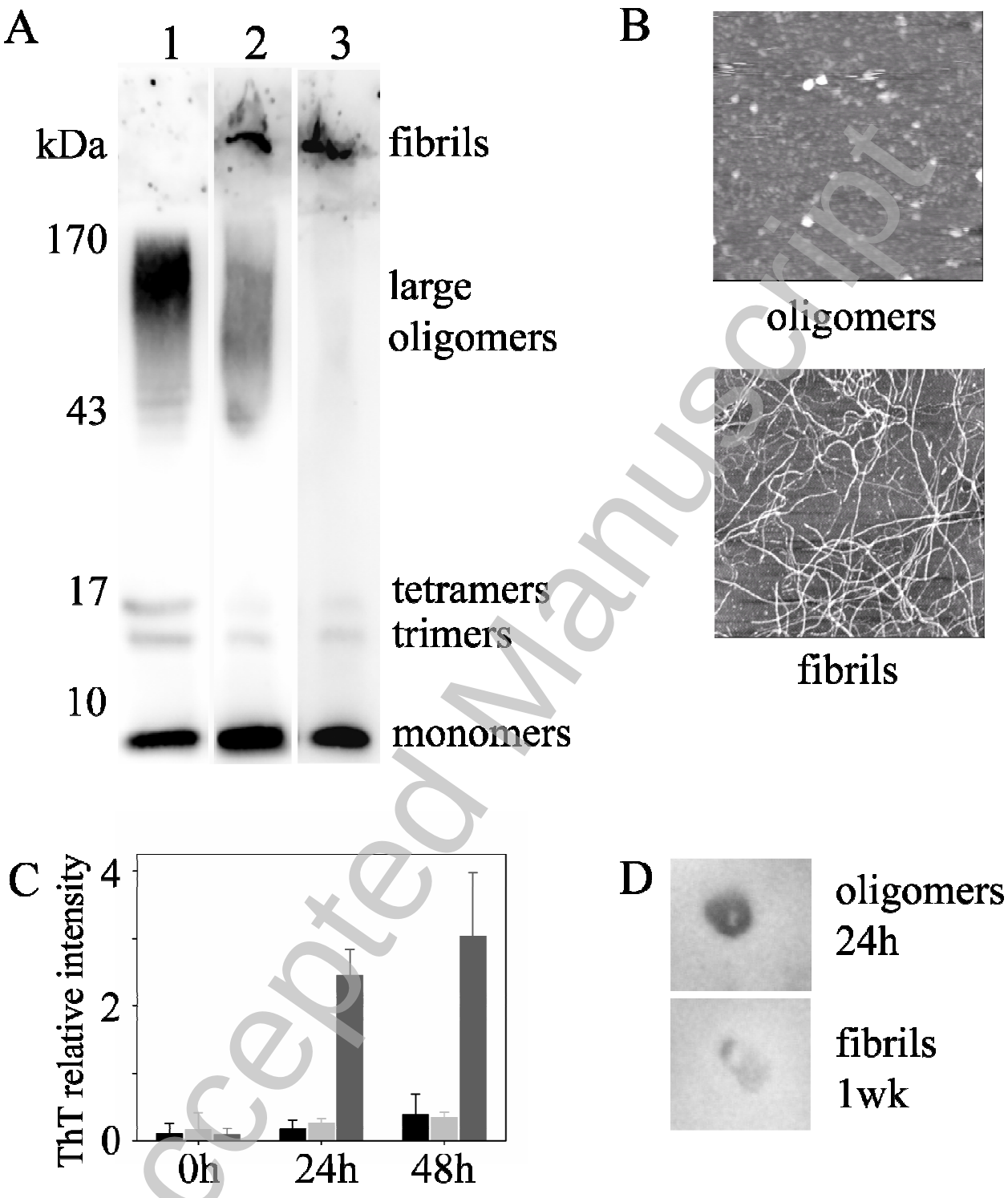

Figure 1

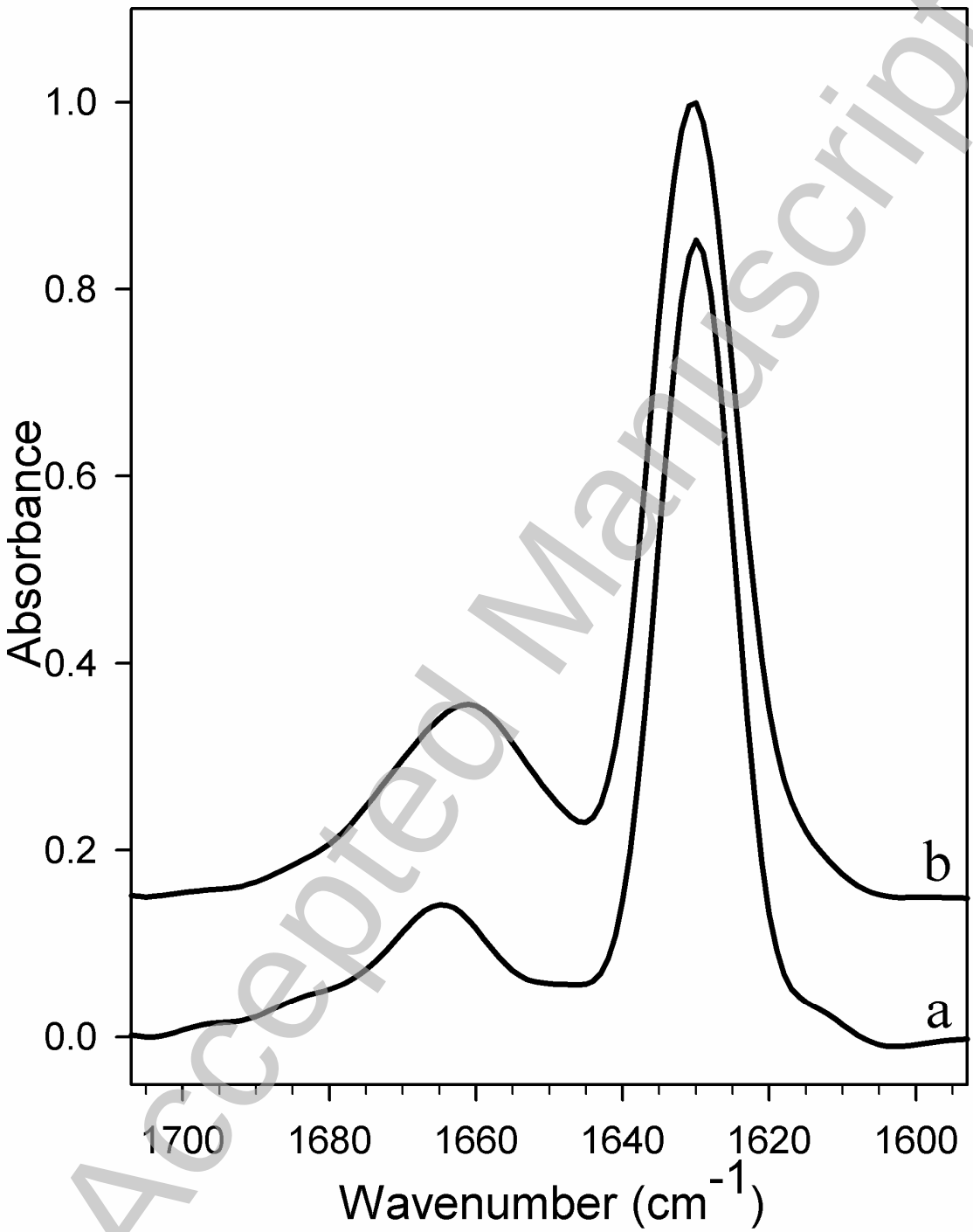

Figure 2

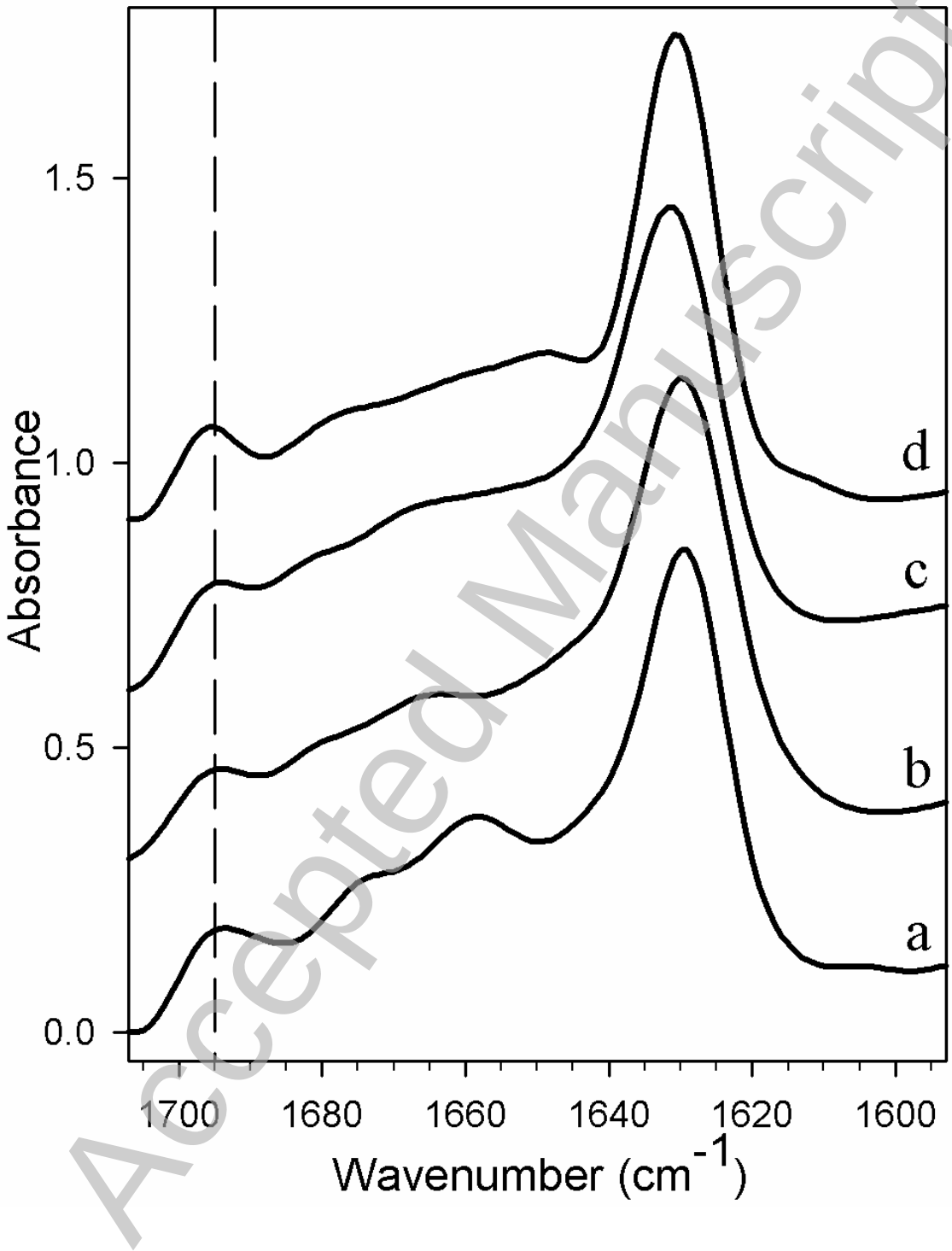

Figure 3

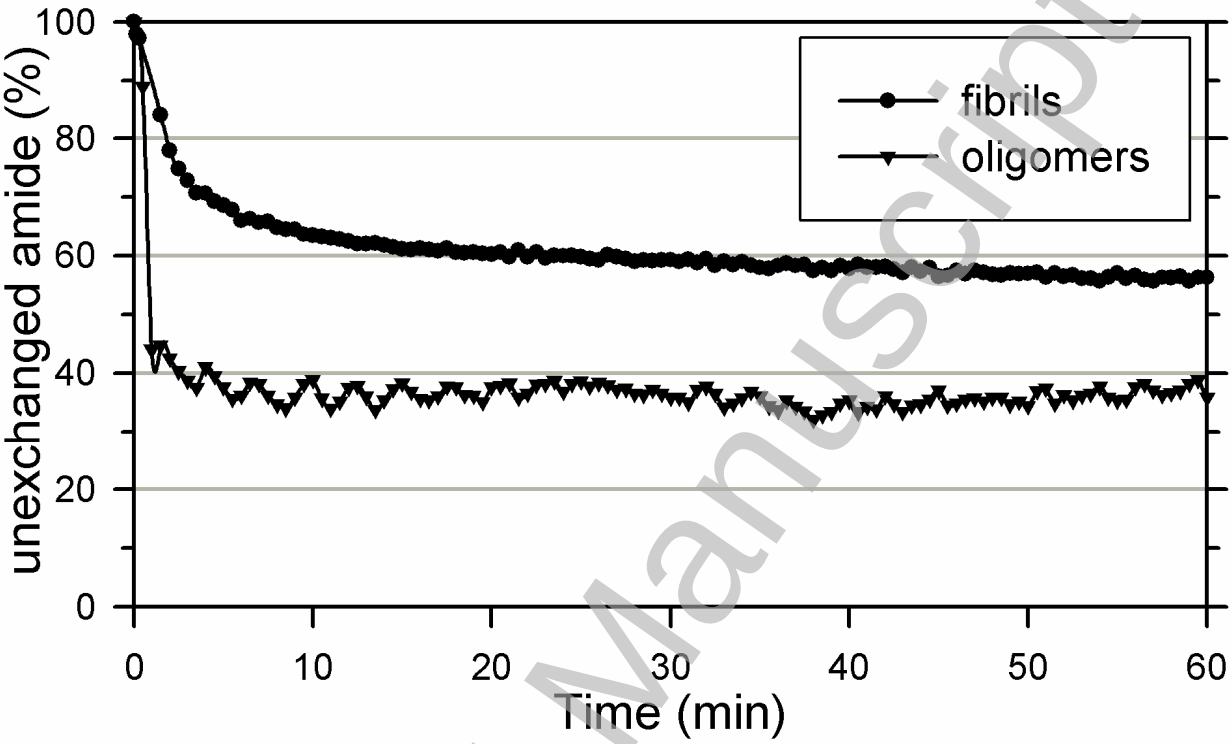

Figure 4

Figure 5

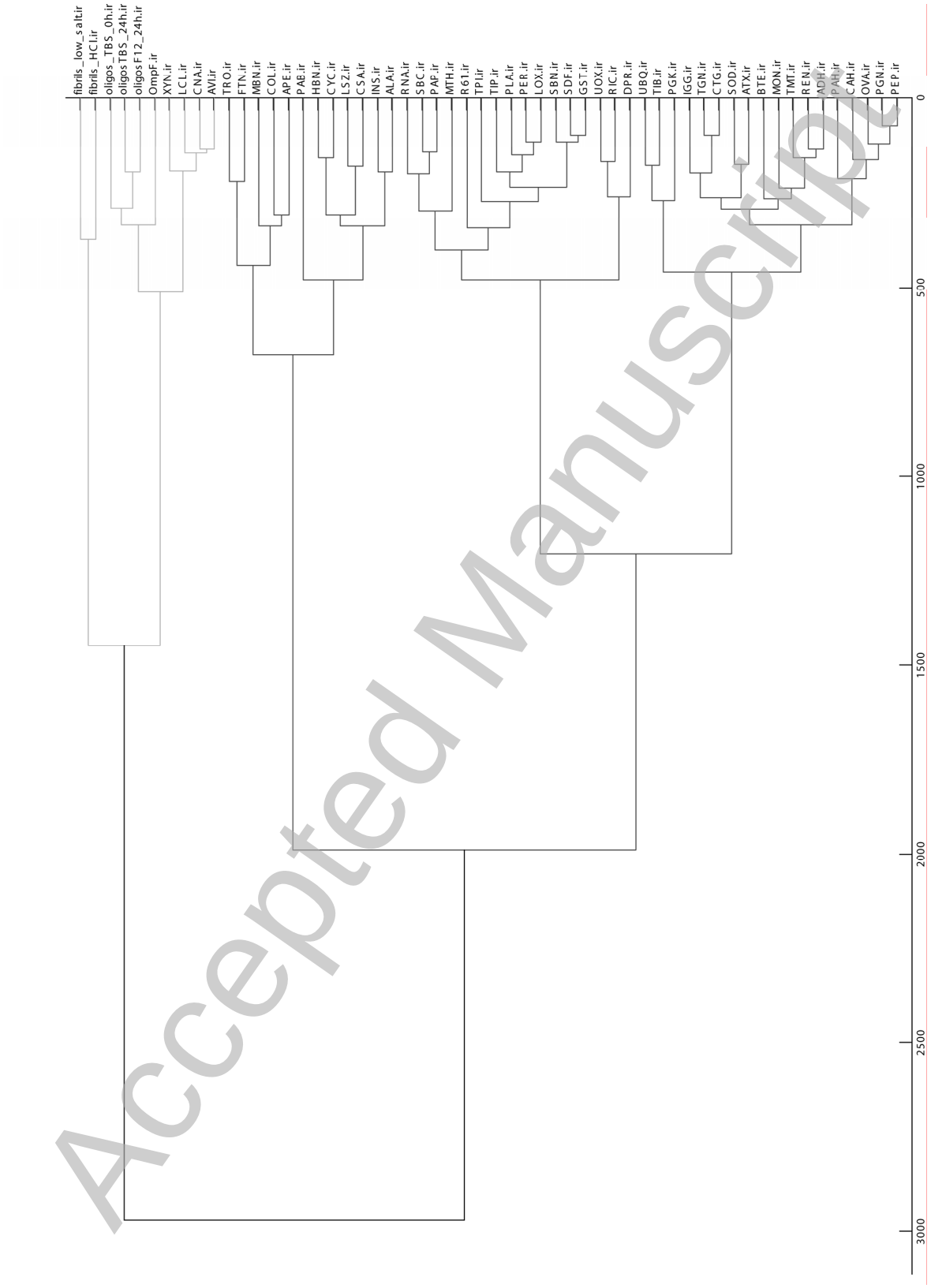

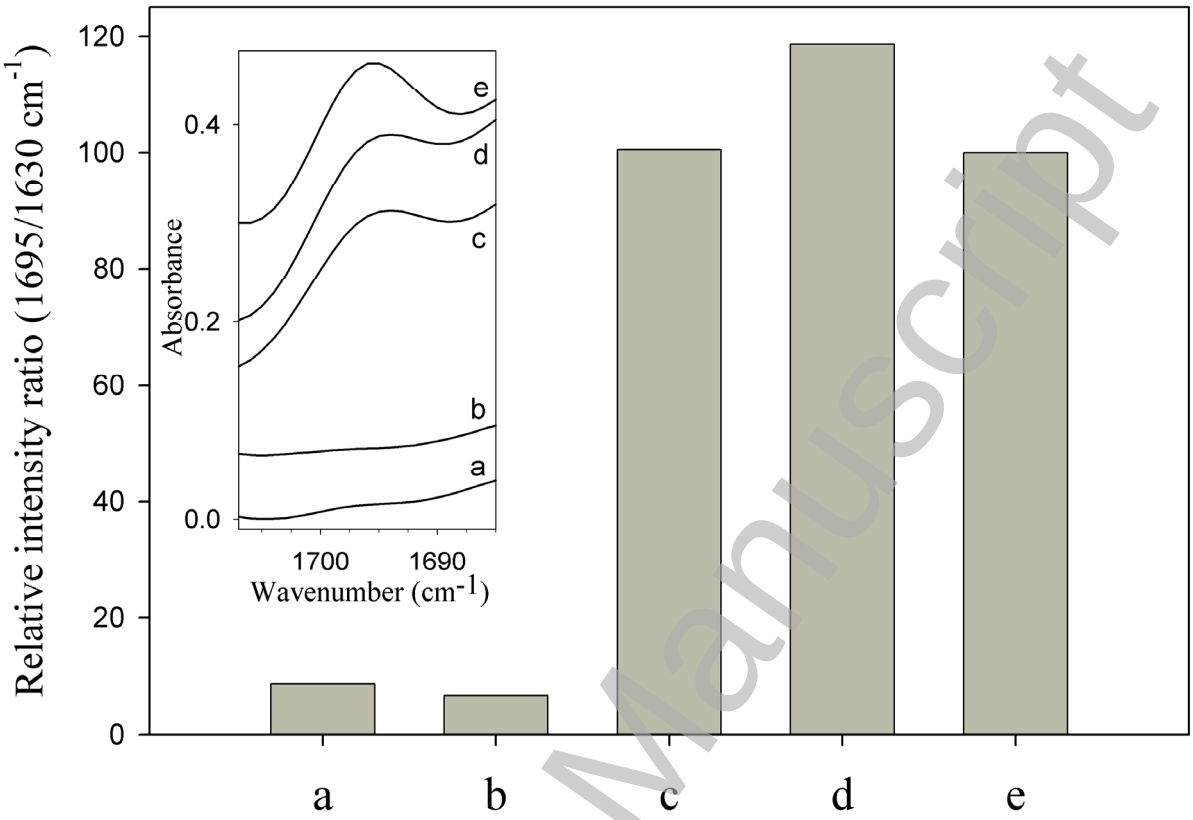

Figure 6

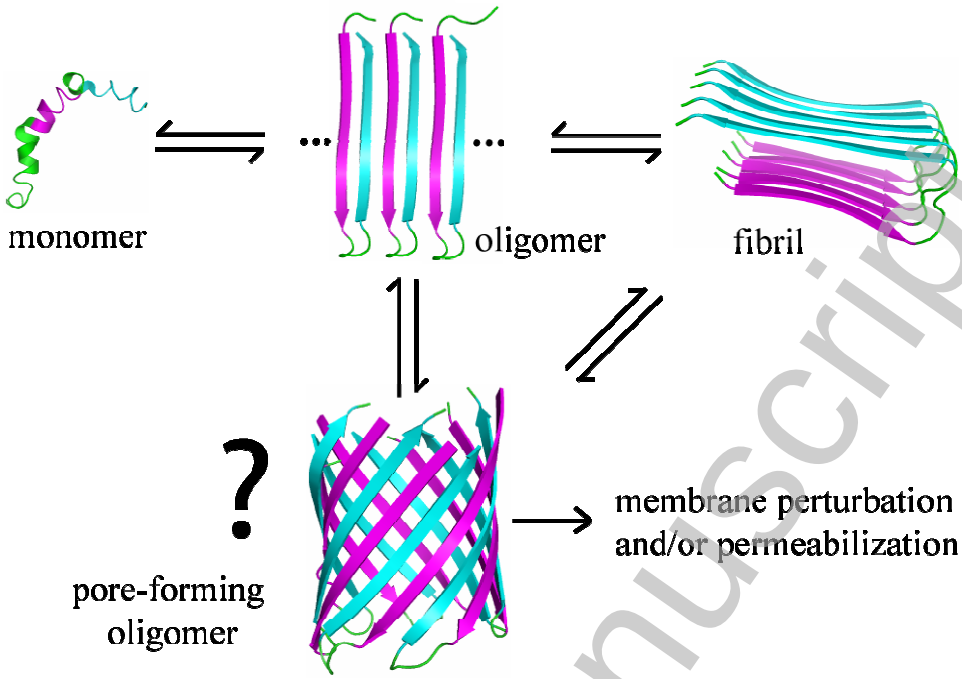

Figure 7